A New Program to Design an Alpha-Type Stirling Engine Using Elbow-Bend Transposed-Fluids Heat Exchangers

برنامج جديد لتصميم محرك استرلنج طراز ألفا باستخدام المبادلات الحرارية على شكل الكوع ذات الموائع المبدلة

A.A. El-Ehwany*, G.M. Hennes*, E.I. Eid** and E. El-Kenany***

* Mech. power Dept., Faculty of Engineering, Ain Shams University, Cairo, EGYPT.
** Mech. Dept., Faculty of Industrial Education, Suez Canal University, Suez, EGYPT.
*** Workers University, Tech. Development Dept., Tanta, EGYPT.

ملخص

في هذا البحث تم تصميم محرك استيرلينج طراز ألفا باستخدام المبادلات الحرارية على شكل الكوع لكل من المسخن والمبرد . المبادل الحراري على شكل الكوع هو مجموعة من الأنابيب تم ترتيبها فى مساحة ربع دائرة إما خطيا أو تداخليا مع اختلاف الخطوة الطولية والعمودية. تم (فى بحث سابق لنفس المؤلفين) تصميم واختبار ثمانية من المبادل الحراري المقترح معمليا فى حالة التدفق المستقر وقد تم صياغة النتائج المعملية فى صورة معادلات وضعية لنقل الحرارة وهبوط الضغط. محرك استيرلينج المقترح فى هذا البحث يتكون من اسطوانتين ومكبسين (متوازيين) متصلان بعمود مرفق واحد ، ويحتوى المحرك على مسخن ومبرد من نوع المبادلات الحرارية على شكل الكوع حيث يتدفق مائع التسخين داخل أنابيب المسخن ووسيط التبريد داخل انابيب المبرد بينما يتدفق غاز دورة المحرك (وسيط التشغيل) حول الأنابيب فى كل منهما. تم إعداد برنامج على الحاسب الآلى لتحليل دورة الغاز فى المحرك فى ضوء نظرية شميت وتم حل الدورة عدديا باستخدام هذا البرنامج وتلى ذلك إدخال أثر انتقال الحرارة والفقد فى الضغط فى الاعتبار. تم تحديد نسبة طول مشوار المكبس الى قطر الأسطوانة لكلا المكبسين الساخن والبارد كما تم تحديد زاوية الطور بين المكبسين ومدى سرعة الدوران الأكثر ملاءمة لأداء المحرك اذا كان غاز دورة المحرك هو النيتروجين. تمت المقارنة بين المحرك المقترح والمحركات الفعلية السابقة فوجد أن المحرك المقترح يولد قدرة نوعية (لكل سنتيمتر مكعب من الحجم المزاح لكل وحدة درجة حرارة فرق بين المصدر والمصب الحرارى) أعلى بالاضافة الى ارتفاع كفاءة المحرك المقترح.

Abstract

In this work, the elbow bend heat exchangers were suggested to be used as a heater and a cooler in an alpha type Stirling engine. Elbow bend heat exchanger is a bank of tubes arranged in a quadrant either in line or staggered with different normal and parallel pitches. Eight of the suggested heat exchanger of different dimensions were tested experimentally for steady flow (in a previous research by the same authors). The experimental results were correlated for heat transfer and pressure drop. In the present research, two parallel pistons on a common crankshaft alpha Stirling engine was designed to use elbow bend heat exchangers as a heater and a cooler. The heating fluid flows inside the tubes of the heater, the coolant flows inside the cooler tubes, while the gas circuit fluid (working fluid) flows past the tubes in both of them. A computer program was prepared to analyze the working fluid cycle in the vision of Schmidt theory and it was solved numerically by the program. After that the effect of heat transfer and pressure drop were taken into consideration. Upon calculations, the most suitable values of each of the stroke/bore ratio, the crank phase angle between the hot and cold pistons and the speed range were found out for nitrogen as a working fluid. In a comparison between the proposed engine and practical ones by the literature, it was found that the proposed engine delivers higher power per unit swept volume per unit temperature difference between the heat source and sink in addition to higher values of the efficiency.

Key words: Stirling engines, Elbow bend heat exchangers, Alpha Stirling engine.

Introduction

One of the arrangements of the conventional alpha-type Stirling engine consists of two parallel cylinders. The heating and cooling processes may be achieved through the walls of the two cylinders as shown in Fig. (1-a); one for

Accepted December 31, 2009.

heating and the other is for cooling. Another technique of transferring the heat to and from the working fluid is by using two heat exchangers; heater and cooler. The conventional heater and cooler in this case consist of a number of tubes that are bent in the form of a quadrant as shown in Fig.(1-b). The working fluid flows through the tubes and it can be heated by the flowing of a heating fluid past the heater tubes and cooled by passing the coolant past the cooler tubes.

In this paper, eight elbow bend heat exchangers were designed and manufactured to be used as a heater and a cooler in an alpha-type Stirling engine. The geometrical shape of the elbow bend heat exchanger is shown in figures (2-a) and (2-b). The main dimensions of each heat exchanger are presented in Fig. 3. The suggested elbow bend heat exchangers were tested experimentally in a steady flow test rig to investigate their thermal performance individually. The experimental results were expressed as empirical correlations for heat transfer and pressure drop as given in [1].

The empirical correlations were deduced as follows:

$$\overline{Nu_f} = A \times Re_f^B \quad (1)$$

$$f = C_1 \times Re_f^2 + C_2 \times Re_f + C_3 \quad (2)$$

Where the constants; A, B, C_1, C_2 and C_3 are given in [1].

In the present work, referring to Fig. 4, the elbow-bend heat exchanger will be introduced as a heater and a cooler in a twin-piston alpha Stirling engine. The working gas flows past the tube bank of the elbow-bend heater and cooler. In the heater, flue gases or heating fluids flow inside the tubes while the coolant flows inside the tubes of the elbow-bend cooler as well.

Engine

The present work considers that the engine has a bore of 100 *mm* and a wire mesh regenerator. In the vision of Schmidt assumptions [2 and 3], a harmonic variation of expansion and compression spaces is to be assumed, thus the instantaneous volumes of both are:

$$V_E = (\pi/8) D^2 S_E (1 - \cos\phi) \quad (3)$$

$$V_C = (\pi/8) D^2 S_C (1 - \cos(\phi - \alpha)) \quad (4)$$

The total volume of the engine work space is as follows:

$$V_t = V_E + V_C + V_H + V_K + V_R + V_{cl,E} + V_{cl,C} \quad (5)$$

According to Schmidt assumptions, the instantaneous pressure is the same within the engine work space. The engine work space can be divided into three isothermal spaces; compression and cooler spaces at T_C, expansion and heater spaces at T_E and regenerator space at an intermediate temperature T_R which is as follows:

$$T_R = (T_E - T_C) / Ln(T_E / T_C) \quad (6)$$

The charged mass of the gas is:

$$m_{ch} = P_{ch} V_{t,\max} / R T_{ch}$$
$$= p(V_E + V_H + V_{cl,E})/RT_E + p(V_R)/RT_R + p(V_C + V_K + V_{cl,C})/RT_C \quad (7)$$

The instantaneous Schmidt pressure is:

$$p = \frac{m_{ch} R T_E}{\left[(V_E + V_H + V_{cl,E}) + \left[\ln(1/\xi)/(1-\xi)\right](V_R) + (1/\xi)(V_C + V_K + V_{cl,C})\right]} \quad (8)$$

A computer program in the form of a spread sheet was prepared in which the above equations were inserted to find the Schmidt *p-V* diagram represented in Fig. 5. Referring to Fig. 4; and applying the mass conservation equation between the spaces of the engine workspace, [3].

For the expansion space;

$$dm_E / dt = 0.0 - \dot{m}_{E \to H} \quad (9)$$

For the heater space;

$$dm_H / dt = \dot{m}_{E \to H} - \dot{m}_{H \to R} \quad (10)$$

For the regenerator space;

$$dm_R/dt = \dot{m}_{H\to R} - \dot{m}_{R\to K} \quad (11)$$

For the cooler space;

$$dm_K/dt = \dot{m}_{R\to K} - \dot{m}_{K\to C} \quad (12)$$

For the compression space;

$$dm_C/dt = \dot{m}_{K\to C} - 0.0 \quad (13)$$

From the equations (9, 10, 11, 12 and 13); one can find; $m_{E\to H}$, $\dot{m}_{H\to R}$, $\dot{m}_{R\to K}$ and $\dot{m}_{K\to C}$. Hence the instantaneous flow rate and Reynolds numbers through the heater, the regenerator and the cooler were found as:

$$\dot{m}_H = (\dot{m}_{E\to H} + \dot{m}_{H\to R})/2 \quad (14)$$

$$\dot{m}_R = (\dot{m}_{H\to R} + \dot{m}_{R\to K})/2 \quad (15)$$

$$\dot{m}_K = (\dot{m}_{R\to K} + \dot{m}_{K\to C})/2 \quad (16)$$

$$Re_H = \dot{m}_H \times d_H/(\mu_E \times a_{H,\min}) \quad (17)$$

$$Re_R = \dot{m}_R \times d_{hyd,R}/(\mu_R \times a_R) \quad (18)$$

$$Re_K = \dot{m}_K \times d_K/(\mu_C \times a_{K,\min}) \quad (19)$$

Fig. 6 shows the cyclic mass fluctuations via the heater, the cooler and the regenerator during a complete cycle of the engine.

Heater

The inlet temperature of the flue gases was taken 750°C, [4 and 5]. The flue gases flow rate was considered to be constant at ($\dot{m} = 0.1378\ kg/s$) which ensures minimum $Re_g = 5000$. Thus, the heat addition rate is, [6];

$$\dot{Q}_H = N\oint P_E dV_E = A_{H,o}\, U_H\, (T_g - T_E) \quad (20)$$

Where; $1/U_H = 1/h_g A_i + 1/h_H A_o$ (21)

The expansion space temperature T_E which had been calculated from the heater performance was used to calculate the engine performance. The temperature T_E was calculated with the matching of the heater calculations using iteration method, since $Q_H = W_E$.

The pressure drop through the heater is, [7]:

$$\Delta P_H = 1.7 \times [f \times \rho \times v_{\max}^2/2]_H \quad (22)$$

The values of both h_H and f_H were calculated using the correlations (1 and 2). However the value of h_g was calculated from the following correlation, [6];

$$\overline{Nu}_g = 0.023\, Re_g^{0.8}\, Pr_g^{0.4} \quad (23)$$

Regenerator

The regenerator has a horizontal cylindrical shape of 0.1 m diameter, as shown in Fig. 4. It is formed of successive circular layers of stainless steel wire mesh having the same mesh size. The layers are supposed to be homogenously stacked beside each other without a revolving angle. Mesh of $i = 100$ pores/inch and wire diameter of $d_w = 0.112\ mm$ were proposed for the regenerator fabrication. The pressure drop of the gas due to its flow through the regenerator is, [8]:

$$\Delta p_R = \left[f \times (L/d_{hyd}) \times \rho \times v^2/2\right]_R \quad (24)$$

Where; $D_{hyd} = d_w \sqrt{\dfrac{\psi}{1-\psi}}$

$$\psi = 1 - \frac{1000\, i}{25.4} \times \frac{\pi}{4} \times d_w \quad (25)$$

The friction factor, f, is expressed as follows, [8]:

$$\log(f_R) = 1.73 - 0.93 \log(Re_R) \quad \text{for } 0.0 \prec Re_R \le 60 \quad (26)$$

$$\log(f_R) = 0.714 - 0.365 \log(Re_R) \quad \text{for } 60 \prec Re_R \le 1000 \quad (27)$$

$$\log(f_R) = 0.015 - 0.125 \log(Re_R) \quad \text{for } Re_R \succ 1000 \quad (28)$$

The regenerator effectiveness is, [8]:

$$\varepsilon_R = NTU_R/(1 + NTU_R) \quad (29)$$

$$; NTU_R = 2 \times \overline{St}_R \times L_R/d_{hyd,R} \quad (30)$$

And $St_R = 0.595/Re_R^{0.4} \times Pr_R$ (31)

Cooler

The inlet temperature of the cooling water was assumed to be 40°C. The water flow rate was considered to be constant at ($\dot{m} = 0.3462\ kg/s$) which ensures minimum $\mathrm{Re}_w = 5000$. The heat removal rate is, [6];

$$\dot{Q}_K = N \oint P_C\, dV_C$$
$$= A_{K,o}\, U_K\, (T_C - T_w) \qquad (20)$$

Where; $1/U_K = 1/h_{wt} A_i + 1/h_K A_o$ (33)

The compression space temperature T_C which had been calculated from the cooler performance was used to calculate the engine performance. The temperature T_C was calculated with the matching of the cooler calculations using iteration method, since $\dot{Q}_K = \dot{W}_C$.

The pressure drop through the cooler is, [7]:

$$\Delta P_H = 1.7 \times [f \times \rho \times v^2_{\max} / 2]_H \qquad (34)$$

The values of both h_K and f_K were calculated using the correlations (1 and 2). However the value of h_{wt} was calculated using the following correlation, [6];

$$\overline{Nu}_{wt} = 0.023\, Re^{0.8}_{wt}\, Pr^{0.3}_{wt} \qquad (35)$$

The hydraulic losses ΔP_H, ΔP_K and ΔP_R were taken into consideration to get the actual pressure inside the expansion and compression spaces P_E and P_C, that in turn used for calculating both the power and the thermal efficiency.

Power and efficiency

The elliptic p-V diagrams of the expansion and compression spaces when taking the hydraulic losses into consideration are shown in Fig. 7. The indicated power is, [9 and 10]:

$$P = W_{net,cycle} \times N \qquad (36)$$

$$W_{net,cycle} = (W_E + W_C)_{cycle} \qquad (37)$$

$$W_{E,cycle} = \oint P_E\, dV_E = \sum_{i=1}^{i=n} (P_E \times \Delta V_E)_i \qquad (38)$$

$$W_{C,cycle} = \oint P_C\, dV_C = \sum_{i=1}^{i=n} (P_C \times \Delta V_C)_i \qquad (39)$$

The thermal efficiency of the engine is;

$$\eta_{th} = P / \dot{Q}_H \qquad (40)$$

Results and discussion

Two different design approaches were suggested to select the most suitable engine dimensions as ratios of the bore that result in high engine power. The first design approach considers non-equal strokes for both the expansion and compression pistons, while the second one considers equal strokes. The experimental results of the heat exchanger No. (I) were inserted in the computer program of the engine design. The main dimensions of the engine were varied several times to find the engine power and efficiency. By trial and error method, the dimensions and conditions that lead to the best power and efficiency were recorded. The same procedure was done for each heat exchanger. The results are shown in table (1) for the first approach and table (2) for the second approach. Referring to table (1); one can say; the heat exchanger No. (II) is the most suitable candidate as a heater and a cooler for the first design approach. As a consequence; the results will be ongoing discussed when the heat exchanger No. (II) was used as a heater and a cooler in the proposed engine. The working fluid used in the engine is nitrogen and all the calculations were done for a maximum pressure limit of 40 *bar*. The increase in the regenerator length increases both the dead volume and hydraulic losses that in turn reduces the power, so, the most suitable length of the regenerator is about 0.0503 *m* as shown in Fig. 8.

In the typical Stirling engine design, the engine indicated power has a linear proportion with the swept volume in the vision of the classical Schmidt model without hydraulic losses. Furthermore, in the vision of this concept and for the same dead volume, the indicated power increases with the increase of swept volume as the percentage of the dead volume comes down. This is more accentuated in figures (9 and 10) where; the increase in the hot piston stroke or cold piston stroke causes the indicated power to go up although the present model attributes the hydraulic losses. For too long strokes, the charged mass of the working fluid increases and as a consequence the velocity through the heat exchangers increases which increases the hydraulic losses, so, the indicated power comes down. The engine efficiency decreases when increasing any of the strokes for the same reason.

The variation of the phase angle varies the maximum and minimum total volume of the engine work space. This is due to the shift between the crank angles at which the minimum and maximum volumes occur. So, the variation in the phase angle causes a variation in the compression ratio. Fig. 11 shows that the optimum phase angle between the hot and cold pistons of the proposed engine is about 86°. It can be noted that the indicated power increases with the engine speed up to a certain limit as the number of cycles per unit time increases. At higher speeds, the indicated power decreases with increasing the engine speed due to the hydraulic losses and the inadequate heat transfer at higher speed levels. For the proposed engine; the optimum speed is around 500 *rpm* as shown in Fig. 12.

Comparison between the present work and literature

An alpha engine of 1*kW* target with a heat source of 300 °C was tested experimentally by Takeuchi [11] at different engine speeds. The engine has a compression ratio of 1.23 and it developed a power of 805 *W* at 700 *rpm*.

A prototype alpha Stirling engine API-10/250 used a heat source of 300 °C and a heat sink of 20 °C was tested experimentally at different engine speeds by Takeuchi [12]. It generated a power of 10.4 *kW*.

An alpha engine with a heat source of 237 °C and a heat sink of 30 °C was tested experimentally by Isshiki [13] at different speeds and different values of temperature difference. The results showed that the relation between the maximum power and the temperature difference between the heat source and the heat sink is almost linear.

Fig. 13 compares the indicated power per cc per unit temperature differential between the heat source and the heat sink versus engine speed of the present engine with the corresponding actual power of the engines of [11, 12 and 13]. A quite agreement among the present results and those by the literature was more attained. In low speed range, the present engine delivers higher indicated power per cc per ΔT ; this is due to the higher temperature differential of the present engine than that of the three engines which causes adequate heat transfer rates at low engine speeds. However, at high speed range; the inadequate heat transfer rates cause the power to come down. As the present engine has higher ΔT than that of the engines in comparison, the present engine operates at higher efficiency than that of the others as shown in Fig. 14.

NOMENCLATURE

Symbol	Description	Unit	Symbol	Description	Unit
A	Surface area	m^2	Re	Reynolds number	
a	Cross section area	m^2	S	Stroke	m
cc	Cubic centimeter		St	Stanton number	
D	Cylinder bore	m	T	Temperature	K
d	Diameter	m	ΔT	Temperature difference	K
f	Friction factor		t	Time	s
h	Heat transfer coef.	$W/m^2.K$	U	Overall heat transfer coefficient	$W/m^2.K$
i	Wire mesh	*Pores/inch*	V	Volume	m^3
L	Length	m	ΔV	Volume difference	m^3
m	Mass	kg	W	Work	J
$\dot{m}$	Mass flow rate	kg/s	v	Velocity	m/s
N	Speed	*rpm*	α	Phase angle	*rad*
NTU	Number of transfer units		ε	Regenerator effectiveness	
Nu	Nusselt number		ϕ	Crank angle	*rad.*
P	Power	W	η	Efficiency	
Pr	Prandtl number		μ	Viscosity	$kg/m\,s$
p	Pressure	N/m^2	ξ	Temp. ratio $= T_C/T_E$	
Δp	Pressure drop	N/m^2	ρ	Density	kg/m^3
Q	Heat transfer rate	W	ψ	Porosity	
R	Specific gas constant	$J/kg.K$			

Subscripts

Symbol	Description	Symbol	Description
C	Compression space	K	Cooler
ch	Charging	max	Maximum
cl	Clearance	min	Minimum
E	Expansion space	o	Outer conditions
f	Working fluid	R	Regenerator
g	Flue gases	t	Total
H	Heater	th	Thermal
hyd	Hydraulic	w	Wire of the regenerator
i	Inner conditions	wt	Cooling water

Conclusions

The current work is concerned with a somewhat new innovation of an alpha Stirling engine using elbow bend heat exchangers with straight tubes. The elbow bend heat exchangers were integrated with the engine as a heater and a cooler. The experimental results of eight elbow-bend heat exchangers were used in designing the proposed engine. The proposed engine has twin cylinders on a common crankcase and it uses nitrogen as a working fluid at a maximum operating pressure of 40 bars. The main dimensions of the engine that result in higher power were found out. The concluded items of the present trial are:

1- The elbow bend heat exchangers having straight tubes are easy to

manufacture, have long life time, reliable, light weight and quite cheap to be suitable candidates in Stirling machines compared to the conventional heat exchangers having curved tubes.

2- Elbow bend heat exchangers reduce the hydraulic losses but they slightly increase the dead volume when compared with the other heat exchangers used in Stirling machines.

3- Upon calculation, a target of about 9 *kW* at a speed range of 400 *rpm* to 700 *rpm* with nitrogen as a working fluid could be achieved.

4- Even though, the elbow bend heat exchangers can be suggested for gamma, double-acting and free-piston Stirling machines. Moreover, they can be used in other thermal applications.

5- The use of elbow bend heat exchangers in Stirling engine results in higher power and efficiency.

References

1. El-Ehawany, A.A., Hennes, G.M., Eid, E.I., El-kenany, E., "Performance of Elbow-bend Heat Exchangers Having Air Side and Water Tube Bank With Different Arrangements", WASJ 6 (1), (2009), pp. 129-143.
2. Walker G. "Stirling Engines", Oxford: Clarendon Press; 1980.
3. Massey, B.S., "Mechanics of Fluids", Van Nostrand Reinhold (U.K.) Co. Ltd., 5th Edition, (1983).
4. Chung, W. and Kim, S., "Experimental Study of Heat Input System in Stirling Engine", 7th ISEC, Waseda University, Shinjuku, Tokyo, (1995), pp. 113-118.
5. Podesser, E., "Small Scale Cogeneration in Biomass Furnaces with a Stirling Engine", 8th ISEC, (1997), 97084, Ancona, Italy.
6. Holman, J.P. (2002), "Heat Transfer", Ninth Edition, New York, McGraw-Hill Inc.
7. Tsuchiya, K., Uchida, S., Hatanaka, T., Okamura, N. and Fujii, I., "Non-Linear Pressure Drop in Heat Exchanger Element under Periodic Flow Condition", 7th ISEC, Waseda University, Shinjuku, Tokyo, (1995), pp. 83-88.
8. Tanaka, M., Yamashita, I. and Chisaka, F., "Flow and Heat Transfer Characteristics of the Stirling Engine Regenerator in an Oscillating Flow", JSME Int. Jour., Series II, Vol. 33, No. 2, (1990), pp. 283-289.
9. Kongtragool, B. and Wongwises, S., "Technical note: Thermodynamic Analysis of a Stirling Engine Including Dead volumes of Hot Space, Cold Space and Regenerator", Renewable Energy 31 (2006), pp. 345–359.
10. Reader, G.T. and Hooper, C., "Stirling Engines", University Press, Cambridge, U.K., (1983), pp. 341-359.
11. Takeuchi, M., Suzuki, S., Abe, Y. and Kitahara, A., "Development of 1 kW Class Low Temperature Differential Indirect Heating Stirling Engine using Alpha-Type Mechanism", 13th ISEC, Waseda University, Tokyo, Japan, (2007), 38-41.
12. Takeuchi, M., Abe, Y., Suzuki, S., Nakaya, Z. and Kitahara, A., "Development Of 10 kw Class Low Temperature Differential Indirect Heating Stirling Engine Using Alpha - Type Mechanism", 13th ISEC, Waseda University, Tokyo, Japan, (2007), 42-45
13. Isshiki, S., Sato, H., Konno, S., Shiraishi, H., Isshiki, N. and Fujii, I., "The Experimental Study of an Atmospheric Stirling Engine Using Pin-Fin Arrays Heat Exchangers", 13th ISEC, Waseda University, Tokyo, Japan, (2007), 12-17.

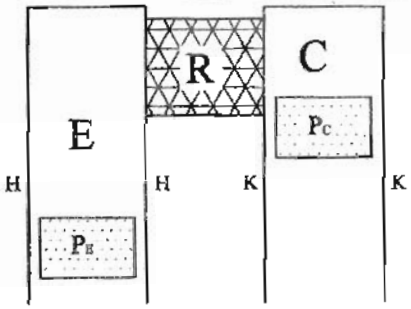

C: Compression space,
E: Expansion space,
H: Heater,
K: Cooler,
P_c: Compression space piston,
P_E: Expansion space piston,
R: Regenerator.

Fig. 1-a. Alpha-type Stirling engine with heating and cooling through the cylinder walls.

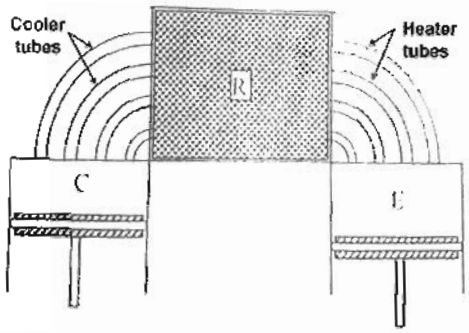

Fig. 1-b. Alpha type Stirling engine with curved-tubes heater and cooler.

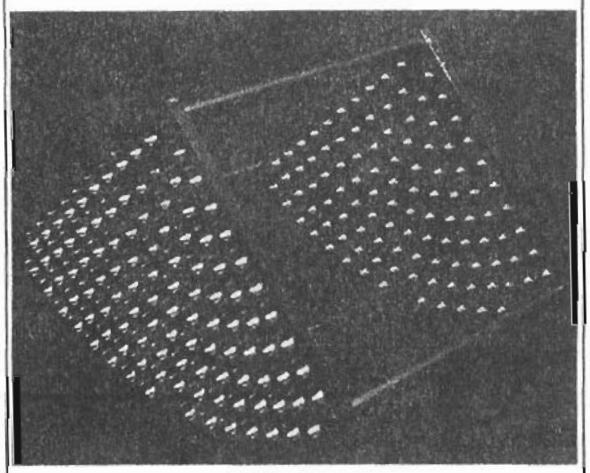

Figure (2-a), Elbow-bend heat exchanger during assembly.

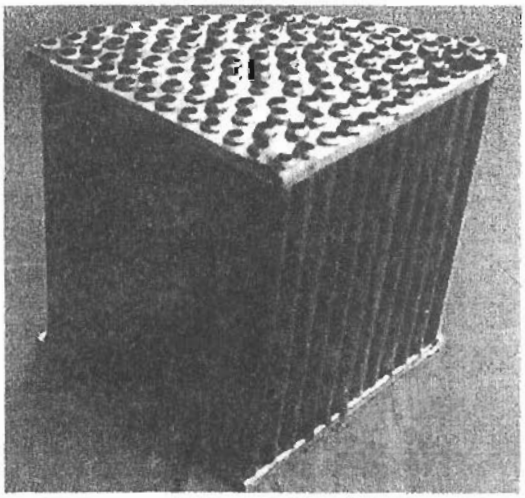

Figure (2-b), Elbow-bend heat exchanger after assembly.

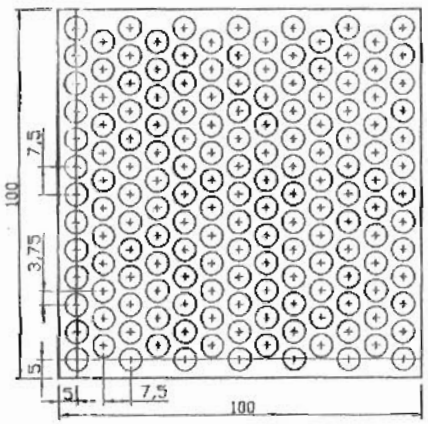

Fig. 3-a. Heat exchanger No.(I), 163 tubes, (Staggered arrangement).

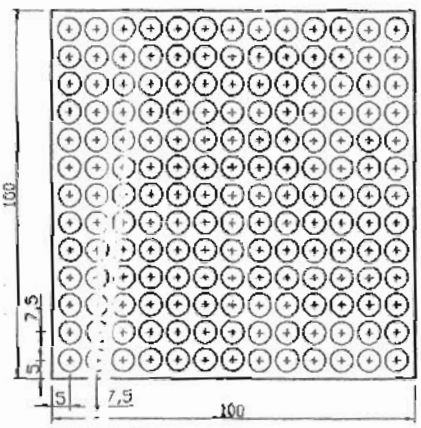

Fig. 3-b. Heat exchanger No.(II), 169 tubes, (In-line arrangement).

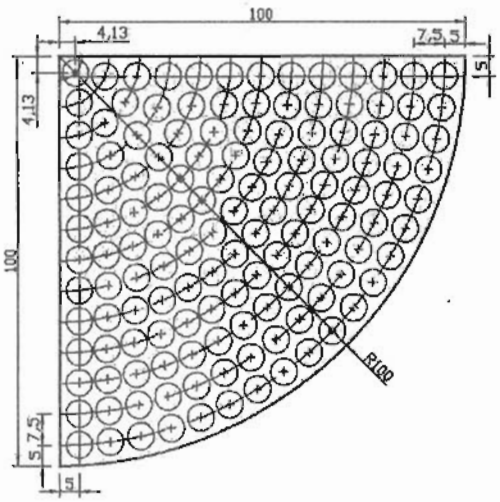

Fig. 3-c. Elbow-bend heat exchanger No. (III), 136 tubes, (Circular arrangement).

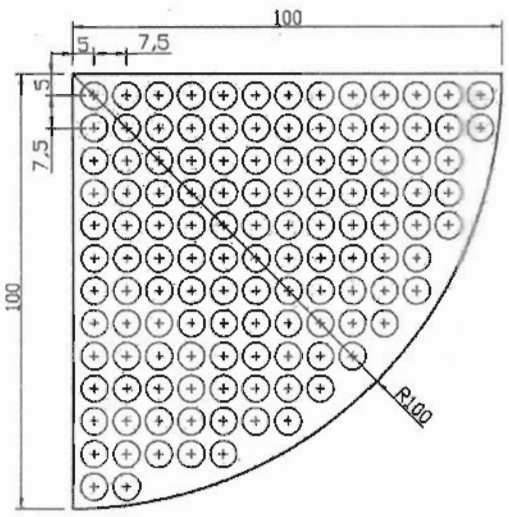

Fig. 3-d. Elbow-bend heat exchanger No. (IV), 125 tubes, (In-line arrangement).

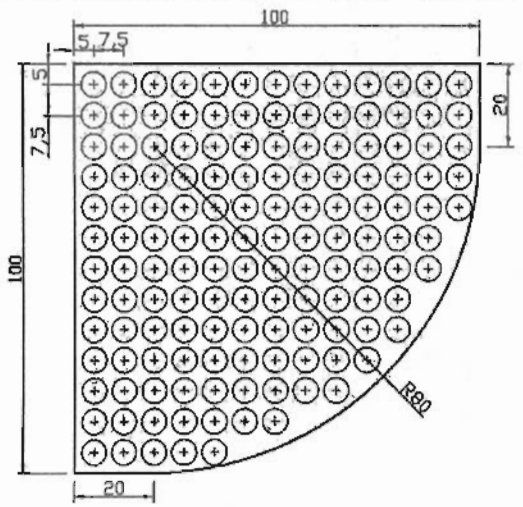

Fig. 3-e. Elbow-bend heat exchanger No. (V), 142 tubes, (In-line arrangement).

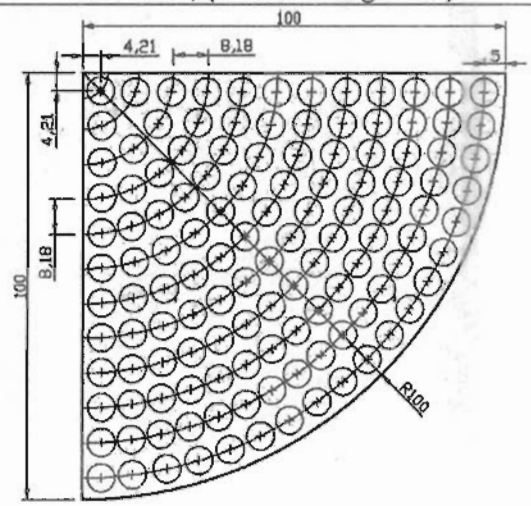

Fig. 3-f. Elbow-bend heat exchanger No. (VI), 124 tubes, (Circular arrangement).

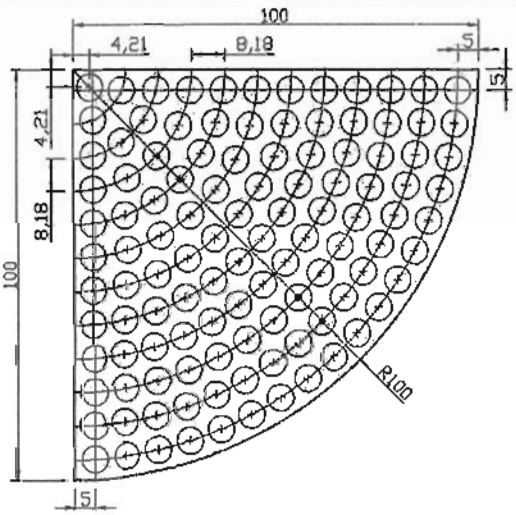

Fig. 3-g. Elbow-bend heat exchanger No. (VII), 113 tubes, (Circular arrangement).

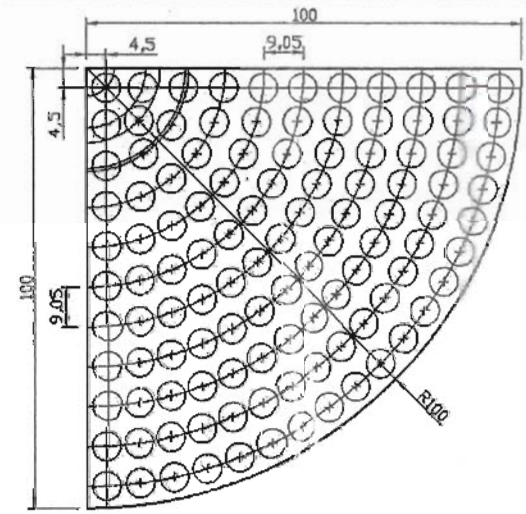

Fig. 3-h. Elbow-bend heat exchanger No. (VIII), 111 tubes, (Circular arrangement).

Figure (3), Specifications of the eight elbow-bend heat exchangers.

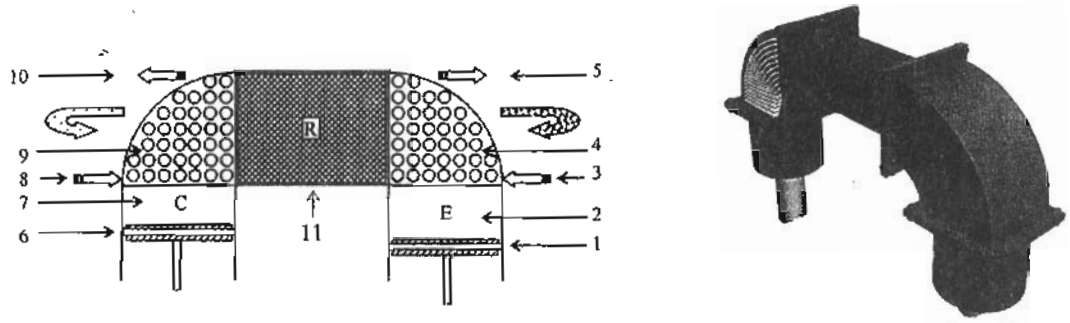

1- Hot piston
2- Expansion space
3- Flue gases inlet
4- Elbow bend heater
5- Flue gases outlet
6- Cold piston
7- Compression space
8- Coolant inlet
9- Elbow bend cooler
10- Coolant outlet
11- Regenerator

Fig. 4. Scheme of the work spaces of the proposed alpha-type Stirling engine.

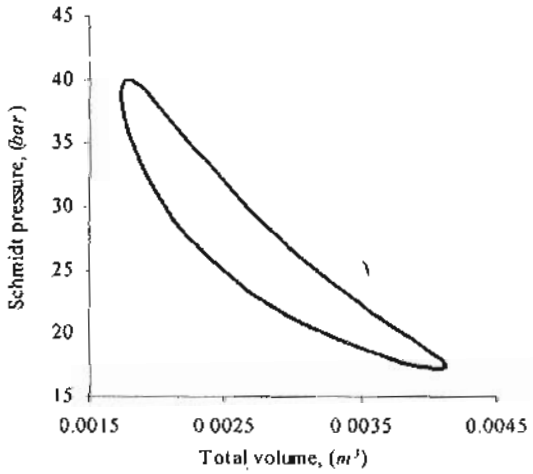

Fig. 5. Schmidt *p-V* diagram.

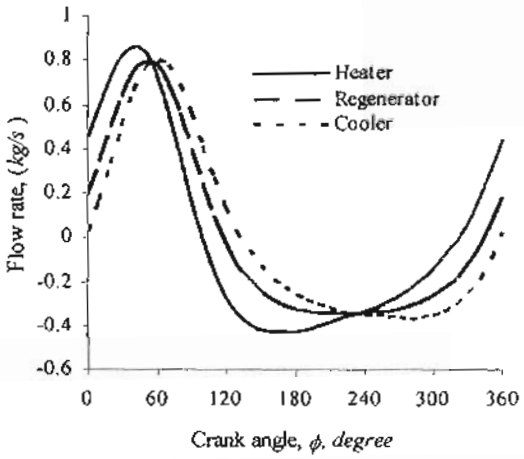

Fig. 6. Cyclic flow rate through heater, regenerator and cooler.

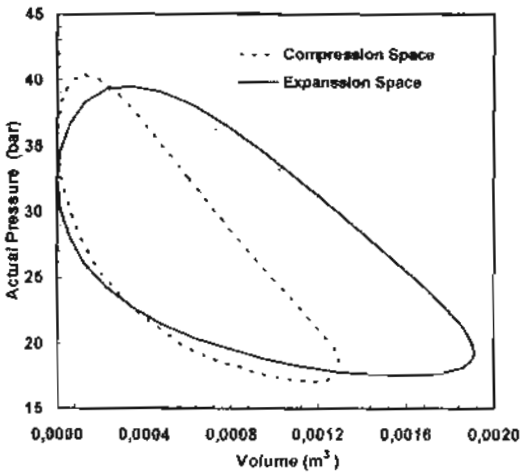

Fig. 7. *p-V* diagrams for both expansion and compression spaces.

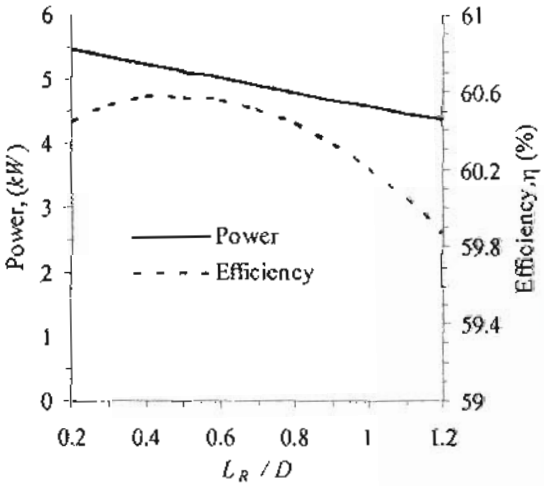

Fig. 8. Indicated power and efficiency versus the regenerator length for $S_E / D = S_C / D = 1.0$.

Table (1), Maximum power developed for each elbow-bend heater and cooler for first design approach (non-equal strokes).

Heat exchanger no.	I	II	III	IV	V	VI	VII	VIII
L_R / D	0.505	0.503	0.503	0.505	0.505	0.506	0.506	0.506
S_E / D	2.404	2.437	1.998	1.989	2.117	2.096	2.148	2.337
S_C / D	1.6	1.66	1.5	1.5	1.55	1.5	1.50	1.55
α (degree)	96	86	112	106	106	110	110	106
N, (rpm)	491	500	512	500	494	510	505	492
Power (kW)	8.175	8.729	7.456	7.270	7.592	7.507	7.533	8.161
η, (%)	42.470	43.660	42.040	42.180	42.320	41.700	42.190	42.860
ε_R, (%)	97.882	97.938	97.844	97.920	97.882	97.831	97.819	97.801
T_E, (°C)	367.2	368.5	375.4	377.9	376.6	367.4	369.6	358,4
T_C, (°C)	74.1	65.4	80.3	80.4	77.1	77.9	75.5	67.9
T_E-T_C, (°C)	293.1	303.1	295.1	297.5	299.5	289.5	294.1	290.5
η_{Carnot}	45.78	47.24	45.51	45.71	46.11	45.21	45.76	46.02
T_{g2}, (°C)	626.7	621.9	636.5	639.8	635.2	634.8	635.8	628.1
ε_H, (%)	30.3	31.4	28.6	27.9	29.0	28.5	28.5	29.5
m_f (g)	54.04	51.05	47.79	48.25	50.68	50.56	52.98	54.31
p_{ch}, (bar)	11.847	10.877	12.888	12.54	12.564	12.976	13.19	12.722
V_{dead}, (cc)	862.254	905.023	509.817	639.37	662.799	598.498	663.393	688.25
V_{swept}, (cc)	3144.73	3217.78	2747.32	2740.25	2880.06	2824.29	2865.13	3061.48
V_t, (cc)	4006.99	4122.8	3257.14	3379.62	3542.85	3422.79	3528.53	3749.73
V_{dead}, (%)	33.94	32.03	33.78	34.67	34.39	34.44	35.38	33.63
Specific power (Watt / cc)	2.6	2.71	2.71	2.65	2.64	2.66	2.63	2.67

Table (2), Maximum power developed for each elbow-bend heater and cooler for second design approach (equal strokes).

Heat exchanger no.	I	II	III	IV	V	VI	VII	VIII
L_R / D	0,505	0,503	0,503	0,505	0,505	0,506	0,506	0,506
S / D	2	2,06	1,77	1,77	1,85	1,815	1,842	1,957
α (degree)	96	86	109	106	102	107	106,5	101
N, (rpm)	498	500	505	500	495	507	504	494
Power (kW)	8,098	8,650	7,408	7,127	7,515	7,443	7,478	8,091
η, (%)	42,28	43,41	42,13	38,43	41,97	41,49	41,79	42,39
ε_R, (%)	97,943	97,952	97,890	97,922	97,923	97,870	97,86	97,853
T_E, (°C)	363,27	366,97	374,44	375,78	372,77	364,03	364,29	353,04
T_C, (°C)	72,64	64,35	79,87	79,32	76,80	77,32	75,22	67,61
T_E -T_C, (°C)	290,63	302,62	294,57	296,47	295,97	286,71	289,07	285,44
η_{Carnot}	45.68	47.29	45.50	45.69	45.83	45.01	45.36	45.59
T_{g2}, (°C)	626.5	622.3	637.5	639.9	635.4	635.2	635.5	627.8
ε_H,(%)	29.9	31.0	28.2	27.8	28.5	28.0	28.0	29.0
m_f (g)	53.75	50.81	46.63	48.01	49.24	49.44	51.73	52.54
p_{ch}, (bar)	11,859	10,833	12,430	12,413	12,064	12,586	12,767	12,223
V_{dead}, (cc)	839,72	884,32	515,03	616,88	679,67	599,49	665,82	701,59
V_{swept}, (cc)	3141,59	3235,84	2780,31	2780,31	2905,97	2851,00	2893,41	3074,05
V_t, (cc)	3981,31	4120,16	3295,34	3397,19	3585,65	3450,48	3559,23	3775,64
V_{dead}, (%)	34,16	32,05	33,39	34,49	33,98	34,16	35,07	33,40
Specific power (Watt / cc)	2,58	2,67	2,66	2,59	2,59	2,61	2,58	2,63

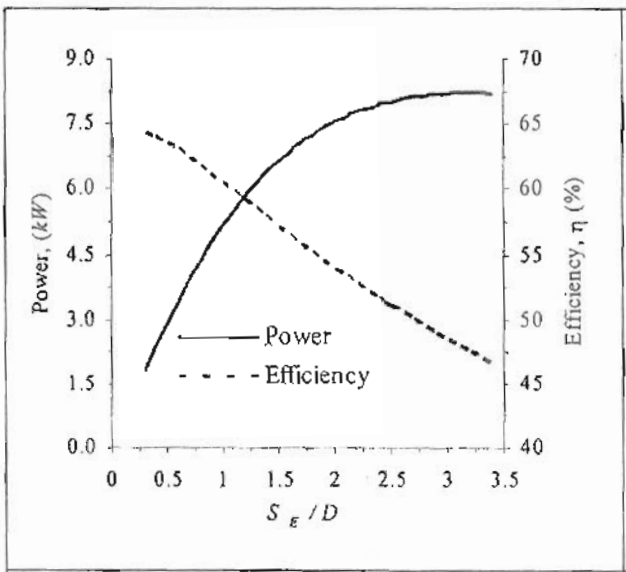

Fig. 9. Indicated power and efficiency versus hot piston stroke for $S_C / D = 1.0$ and $L_R / D = 0.503$.

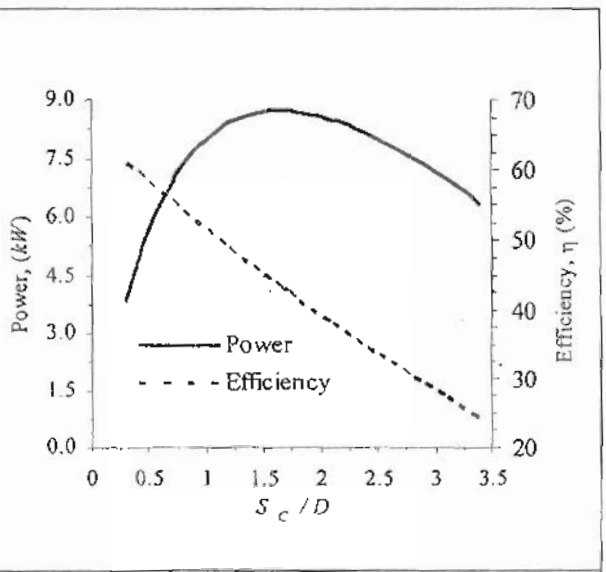

Fig. 10. Indicated power and efficiency versus cold piston stroke for $S_E / D = 2.437$ and $L_R / D = 0.503$.

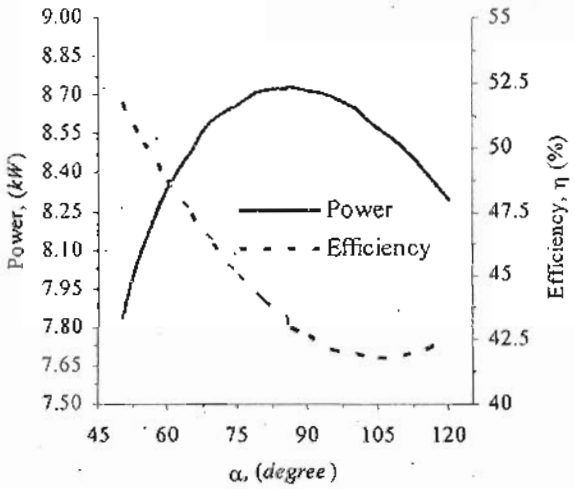

Fig. 11. Power and efficiency versus α for $S_E / D = 2.437$, $S_C / D = 1.66$ and $L_R / D = 0.503$.

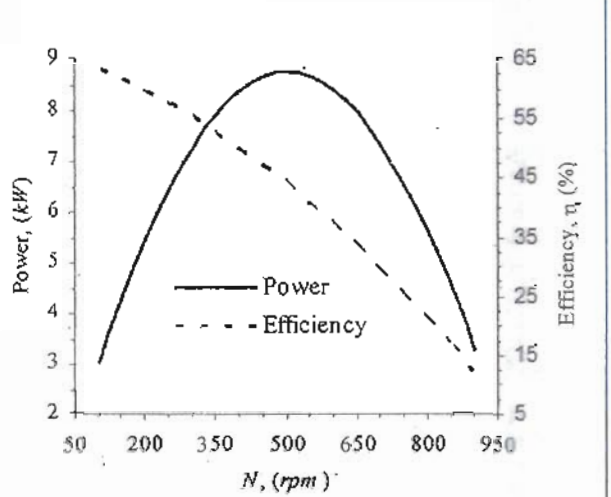

Fig. 12. Power and efficiency versus N for $\alpha = 86°$, $S_E / D = 2.437$, $S_C / D = 1.66$ and $L_R / D = 0.503$.

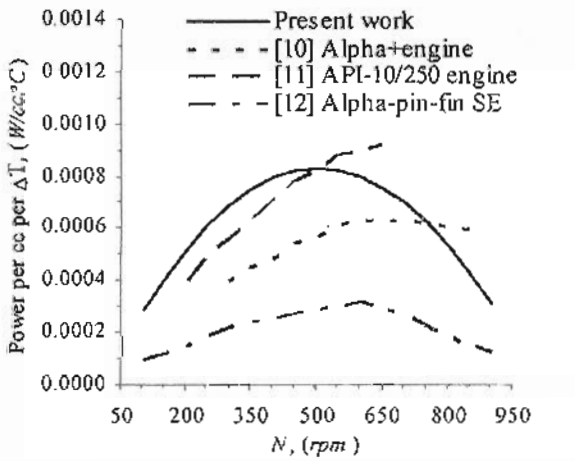

Fig. 13. Comparison of the power per cc per ΔT between source and sink temperatures of the present work and those by the literature.

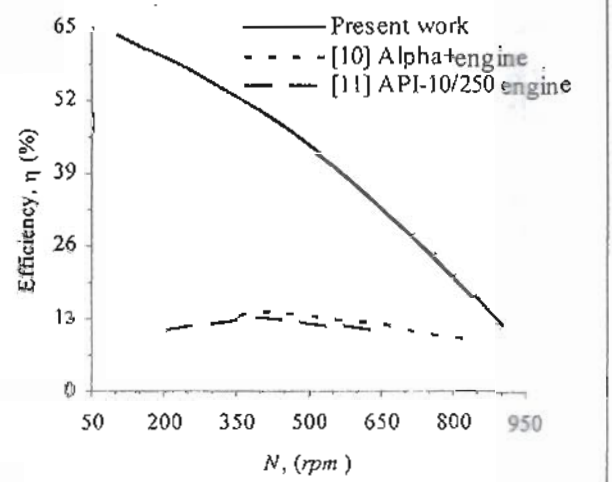

Fig. 14. Comparison of the efficiency of the present work and those by the literature.